The kinetics of precipitation in Al-Zn-Mg-Cu alloy

Y. LIU*, D. M. JIANG, W. J. LI
School of Materials Science and Engineering, Harbin Institute of Technology, Harbin 150001, China

The kinetics of precipitation in supersaturated solid solution of 7050 aluminum alloy was investigated by a combination of differential scanning calorimetric (DSC) techniques with Johnson-Mehl-Avrami (JMA) equation. The results demonstrated that, the activation energy of GPI 353 K, η' phase 492 K and η phase 510 K were 103.8, 195.1 and 571.9 kJ/mol, respectively. The constant of k_0 were 10^{13}, 4.8×10^{16} and 7.9×10^{56} /s, respectively. The equations of the corresponding kinetics were gained at the same time.

(Received July 11, 2015; accepted November 25, 2016)

Keywords: Differential scanning calorimetric, 7050 alloy, Kinetics, Activation energy

1. Introduction

7xxx series alloys have been considered in a wide variety applications as in aviation and aerospace industry for several decades, due to their excellent mechanical properties, high thermal and electrical conductivity, and superior resistance to corrosion [1-7]. The phenomenon of age-hardening in aluminum alloys was discovered by Alfred Wilm in the first decade of the century and led to the development of the well-known duralumin [8]. The strength of Al-Zn-Mg-Cu alloy is mainly controlled by precipitation during aging, which occurs through a complex sequence as follows: supersaturated solid solution (SSS) → Guinier-Preston (GP) zones → metastable η' → stable η ($MgZn_2$) [9]. GP zones are generally accepted as precipitates formed below about 120 ^oC and the early stages of artificial aging [9,10]. In combination with the evolution of quenched-in excess vacancies, these precipitates strongly influence the subsequent precipitation of the metastable η' phases, which are commonly considered as the main hardening phase in 7xxx series alloys [10]. The partly coherent η' phases are generally accepted as precipitates formed between 120 and 150 ^oC. The precipitation of non-coherent η phase takes place with the composition of $MgZn_2$ between 150 and 300 ^oC [9]. The aging behaviour and the precipitation process of these alloys have been assessed by various methods, such as hardness, resistivity measurement, calorimetry and X-ray diffraction study [11]. Since any change in composition, processing and aging practices, etc. can affect the precipitation hardening behavior and lead to complex microstructural conditions, it is still essentially required to study the microstructural features and the hardening process of the alloy for further understanding and correlating the structure-property relationship [11,12]. Since the morphology, sizes and distributions of precipitates directly affect the mechanical properties of alloy, the organizational transformation kinetics parameters of the precipitation process enable us to control aging process and obtain the desired properties of alloys.

Considering the limitations in quantitative transmission electron microscopy (TEM) method, i.e. susceptibility to errors and time-consuming technique, differential scanning calorimetric (DSC) can conveniently be utilized as a supplement to TEM studies to achieve rapid and qualitative description of solid-state phase transformation/precipitation in aluminum alloys [11,13-17]. Generally, DSC is a technique particularly well suited to characterize the kinetics of precipitation and dissolution reactions in aluminum alloys under non-isothermal conditions and resistivity measurements under isothermal conditions [11,18-23]. Hence, a key aim of this work was to discuss the sequences of solid state precipitation and dissolution reactions of a Al-Zn-Mg-Cu alloy from the DSC thermograms. Our present contribution contains various calculated kinetic parameters based upon the kinetics theory of Johnson-Mehl-Avrami relate the transformed volume fraction of the precipitation with the aging time, such as activation energy, frequency factor and the transformation function.

2. Experimental procedure

The material used in this study was rolled 7050 45 mm thick plate (5.85 Zn, 2.28 Mg, 2.13 Cu, 0.094 Zr, 0.055 Fe, 0.019 Mn, 0.041 Si and balance Al, in wt.%), provided by Northeast Light Alloy Co., Ltd.. Differential scanning calorimetry (DSC) was carried on different samples using a DSC Q2000 V24.9 Build 121 instrument. Specimen for DSC analysis was punched into small discs with thickness of 1 mm and a diameter of 4 mm. The quality of the specimen was smaller than 30mg. Specimens were submitted to DSC under a Nitrogen atmosphere with scanning rates of 5K/min.

3. Results and discussion

3.1. Kinetics theory

The discontinuous precipitation kinetics can be obtained by Johnson-Mehl-Avrami (JMA) equation of isothermal transformation kinetics:

$$\xi = 1 - \exp(kt^n) \quad (1)$$

ξ is the volume fraction of the initial material transformed at t time, n is the Avrami exponent(the exponent which reflects the nucleation rate and the growth morphology) and k is the reaction rate constant, which an Arrhenian temperature dependence is usually assigned:

$$k = k_0 \exp[-Q/(RT)] \quad (2)$$

Q is the activation energy for the crystallization reaction, R is the universal gas constant (8.314J/mol K), T is the isothermal temperature and k_0 is the frequency factor.

The volume fraction of precipitation and dissolution reactions with temperatures can be calculated by measuring the net area under a DSC trace. During the DSC run, the heat effects, Q(T), between the initial temperature T_i and temperature T of a peak is associated with the area under the peak between initial temperature T_i and temperature T. Hence, the volume fraction of precipitation and dissolution reactions, i.e. the amount of phase precipitated or dissolved at a given temperature range, can be given by:

$$\xi = S(T)/S(f) \quad (3)$$

The derivation of equation (1) gives the volume fraction of precipitation:

$$d\xi / dt = k^{1/n} f(\xi) \quad (4)$$

$$d\xi / dt = (d\xi / dT)(dT / dt) = \varphi(d\xi / dT) \quad (5)$$

φ is heating rate.

We can get the activation energy by simultaneous Equation (2) (4) (5),

$$\ln[(d\xi / dT)(\varphi / f(\xi))] = \ln k_0 - (Q/R)(1/T) \quad (6)$$

n is chosen based on growth mechanism by long-range diffusion controlled.

Therefore, a plot of $\ln[(d\xi / dT)(\varphi / f(\xi))]$ vs (1/T), under different heating rates, will give a straight line of slope (-Q/R) from which the value of activation energy Q and frequency factor k_0 can be determined.

3.2. DSC analysis

DSC curve calibrated with pure (99.999%) Al for as-quenched 7050 specimen was shown in Fig. 1(a). In the case of age hardenable aluminum alloys, normally, the formation of precipitates is an exothermic process whilst their dissolution is an endothermic process [11,24,26,27]. The peak temperature for the precipitation represents the temperature at which the two factors, i.e. the fall of the driving forces for the continued precipitation (i.e. the decrease of supersaturation with the rise of temperature during DSC run) and the increase of diffusivity with the increase of temperature which results in competing to reach a maximum precipitation rate [11]. In DSC curve with scanning rates of 5K/min, three distinct exothermic peaks from A to C can be observed in the temperature range from 300 to 550K. It was reported that there are two types of GP zones in Al-Zn-Mg-Cu alloys, which are GPI zones and GPII zones. The exothermic peak A at about 350K was associated with the formation of GP zone. While the exothermic peaks B and C from 450 to 550K were associated with the formation of semi-coherent η' precipitates and transformation to η precipitates. Since the reaction temperature of peak B was close to that of peak C, the two peaks were overlapped with each other. Fig. 1(b) showed the separation results of overlap peak to achieve the accurate organizational transformation kinetics relationship.

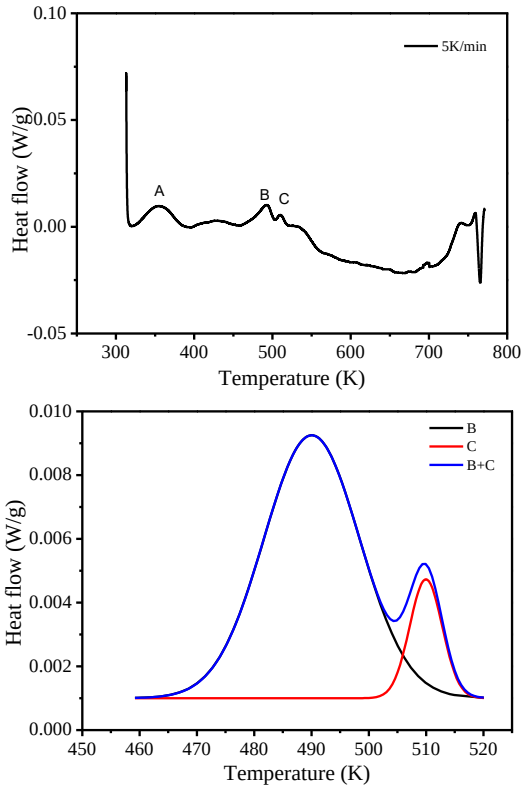

Fig. 1. (a) DSC curve of supersaturated solid solution of 7050 aluminum alloy and (b) Separation results of overlap peak

In combination with DSC curve of supersaturated solid solution and separation results of overlap peak, we can obtain the variations of volume fraction of second-phase particles and precipitation rate with temperatures, shown in Fig. 2. Based on the growth mechanism by long-range diffusion controlled in JMA equation, we select n = 2/3, n = 1, n = 1 as phase transition

constant of GP zone, η' and η phase, respectively [26]. Fig. 3 showed the fitting results of activation energy and the kinetic parameters for the solid state reactions of the 7050 alloy were shown in Table 1.

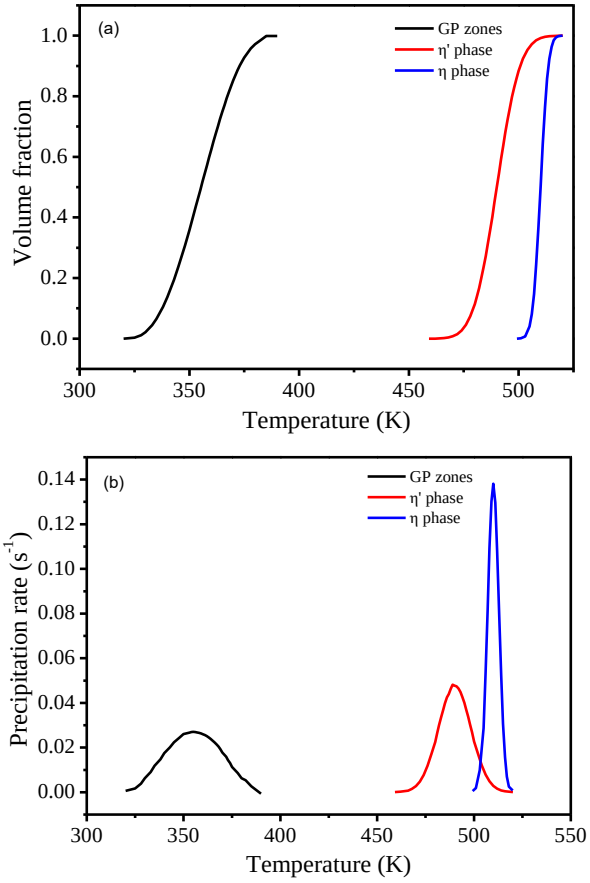

Fig. 2. Variations of volume fraction (a) and precipitation rate with temperature (b)

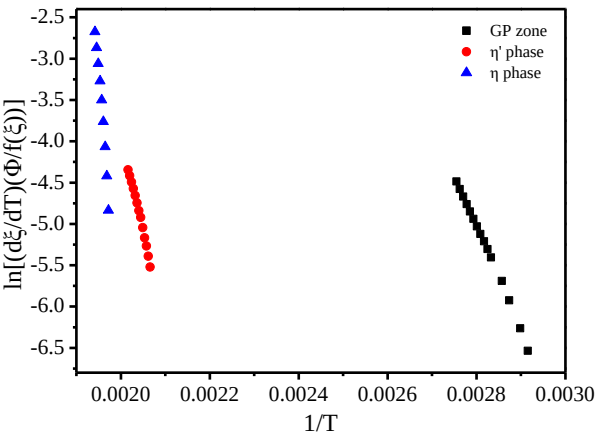

Fig. 3. Determination of activation energy

The quenched aluminum alloy often appears exothermic peaks of GP zone, η' and η in the heating process of DSC curve.

Table 1. Precipitation kinetics of GPI, η′ and η phases

	Peak temperature/K	Q/(kJ·mol^{-1})	k_0/s^{-1}
GPI	353	103.8	10^{13}
η'	492	195.1	4.8×10^{18}
η	510	571.9	7.9×10^{56}

We calculated the kinetic parameters of phase transformation based on the dissolved activation energy of aged alloy during the heating process. The slopes of the three linear straight lines gave the activation energy (Q) for the process. Generally speaking, due to the complexity of the precipitation and dissolution reactions, the calculated activation energy cannot be determined accurately [11]. The activation energy value for the dissolution of GP zones was in good agreement with the values obtained by F. Wei [27]. The higher the degree of alloying, the higher the degree of supersaturation in matrix [28]. Compared with others' investigations, the activation energy of GP zone was higher due to the lower degree of alloying [11-13,16,29]. The activation energy of η' phase was similar with that obtained in Ref. 26. As the temperatures increased, the η formation process will be under the control of thermodynamics and kinetics starting from dynamics controlling. Thus, the activation energy of η phase formation obtained by Kinetic equations will not be determined accurately.

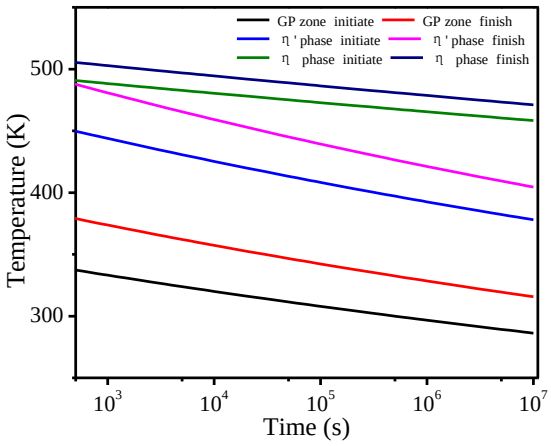

Fig. 4. TTT curve

Based on the precipitation kinetics parameters of GPI, η' and η phases, we can deduce the transformation function as follows:

$$\xi(\mathrm{GP}) = 1 - \exp\{10^{13}\exp[-12484/\mathrm{T}]t^{\frac{2}{3}}\} \quad (7)$$

$$\xi(\eta') = 1 - \exp\{4.8\times10^{18}\exp[-23468/\mathrm{T}]t\} \quad (8)$$

$$\xi(\eta) = 1 - \exp\{7.9\times10^{56}\exp[-68787/\mathrm{T}]t\} \quad (9)$$

While ξ is 5% represented GPI, η' and η phases started to transformation; ξ is 95% represented the finish of transformation. Hence, the TTT curves for phases transformation of 7050 aluminum alloy can be obtained, as shown in Fig. 4.

$$T(GP) = 12484/[\tfrac{2}{3}\ln t + 29.9 - \ln\ln(1-\xi)^{-1}] \quad (10)$$

$$T(\eta') = 23468/[\ln t + 43.0 - \ln\ln(1-\xi)^{-1}] \quad (11)$$

$$T(\eta) = 68787/[\ln t + 131.0 - \ln\ln(1-\xi)^{-1}] \quad (12)$$

4. Conclusions

In this investigation, the DSC thermograms of 7050 alloy taken at 5K/min heating rates exhibited three exothermic peaks which represented the sequence of precipitation reactions, such as the formation of GP zones, the precipitation of η' phase, the precipitation of η phase. From the DSC data, the technique to determine the fraction of transformation, and the method to determine activation energy, frequency factor and the transformation function, were discussed. The values of activation energies of discontinuous precipitation determined using DSC methods based on JMA equation for Al-5.85Zn-2.28Mg-2.13Cu were 103.8, 195.1 and 571.9 KJ/mol, respectively. From the present DSC thermograms, it was difficult to determine the kinetic parameters accurately for the precipitation reaction of η phase because of its thermodynamics and kinetics controlling process.

References

[1] K. Ma, T. Hu, H. Yang, T. Topping, A. Yousefiani, E. J. Lavernia, J. M. Schoenung, Acta Mater. **103,** 153 (2016).

[2] J. T. Jiang, W. Q. Xiao, L. Yang, W. Z. Shao, S. J. Yuan, L. Zhen, Mater. Sci. Eng. A **605**, 167 (2014).

[3] S. Y. Chen, K. H. Chen, P. X. Dong, S. P. Ye, L. P. Huang, J. Alloys Compd. **581**, 705 (2013).

[4] Y. Deng, Z. M. Yin, K. Zhao, J. Q. Duan, J. Hu, Z. B. He, Corrs. Sci. **65**, 288 (2012).

[5] B. Liu, C. Q. Peng, R. C. Wang, X. F. Wang, T. T. Li, Trans. Nonferrous Mat. Soc. China **20,** 1705 (2010).

[6] N. Yazdian, F. Karimzadeh, M. Tavoosi, Indian J. Eng. Mater. Sci. **21**, 30 (2014).

[7] H. F. Wang, J. L. Wang, D. W. Zuo, W. W. Song, X. L. Duan, Indian J. Eng. Mater. Sci. **21**, 557 (2014).

[8] R. Ferragut, A. Somoza, A. Tolley, I. Torriani, J. Mater. Process. Tech. **141**, 35 (2003).

[9] T. Ungar, J. Lendvai, I. Kovacs, J. Mater. Sci. **14,** 671 (1979).

[10] P. Lang, T. Wojcik, E. Povoden-Karadeniz, A. Falahati, E. Kozeschnik, J. Alloy. Compd. **609**, 129 (2014).

[11] K. S. Ghosh, N. Gao, Trans. Nonferrous Met. Soc. China **21,** 1199 (2011).

[12] A. Gaber, M. A. Gaffar, M. S. Mostafa, E. F. Abo Zeid, J. Alloy Compd. **429,** 167 (2007).

[13] R. Deiasi, P. N. Adler, Metall. Trans. A. **8**, 1177 (1977).

[14] R. C. Dorwand, Mater. Sci. Tech-Lond. **15**, 1133 (1999).

[15] J. M. Papazian, Metall. Trans. A. **12**, 269 (1981).

[16] M. Starink, J. International Mat. Review **49**, 191 (2004).

[17] N. Gao, M. J. Starink, T. G. Langdon, Mater. Sci. Tech-Lond. **25,** 687 (2009).

[18] K. S. Ghosh, K. Das, U. K. Chatterjee, Metall. Mater. Trans. A **38**, 1965 (2007).

[19] A. K. Jena, A. K. Gupta, M. C. Chaturvedi, Acta Metall **37**, 885 (1989).

[20] A. K. Gupta, A. K. Jena, M. C. Chaturvedi, Scrip. Metall **22**, 369 (1988).

[21] D. J. Lloyd, M. C. Chaturvedi, J. Mater. Sci. **17**, 1819 (1982).

[22] E. S. Balmuth, Scrip. Metall **18**, 301 (1984).

[23] A. Luo, D. J. Lloyd, A. K. Gupta, W. V. Youdelis, Acta Metall. Mater. **41**, 769 (1993).

[24] A. K. Mukhopadhyay, C. N. J. Tite, H. M. Flower, P. J. Gregson, F. Sale [C]// G. Champier, B. Dubost, D. Miannay, L. Sabetay Proc. 4th Int. Conf. on Aluminum-Lithium Alloys IV. J de Phyique, Suppl. **48**, 439 (1987).

[25] Y. Liu, W. J. Li, D. M. Jiang, J. Mater. Res. **30**, 3803 (2015).

[26] D. Feng, C. X. Shi, G. Z. Liu, Introduction to Materials Science [M]. Beijing: Press of Chemical Industry 541 (2005).

[27] F. Wei, Z. K. Zhao, P. C. Bai, et al. Rare Metal Mat. Eng. **33**, 945 (2004).

[28] J. L. Yang, Y. L. Deng, X. H. Qi, L Wan, X. M. Zhang, J Central South University (Science and Technology) **43,** 2528 (2012).

[29] F. Wei, Z. K. Zhao, P. Y. Liu, T. T. Zhou, Mater. Forum **28,** 75 (2004).

*Corresponding author: ly520208@163.com